Lysophosphatidic Acid Receptor Type 1 (LPA 1) Plays a Functional Role in Osteoclast Differentiation and Bone Resorption Activity

Marion David, Irma Machuca-Gayet, Junichi Kikuta, Penelope Ottewell, Fuka Mima, Raphael Leblanc, Edith E Bonnelye, Johnny Ribeiro, Ingunn Holen, Rùben Lopez Vales, et al.

THE JOURNAL OF BIOLOGICAL CHEMISTRY VOL. 289, NO. 10, pp. 6551–6564, March 7, 2014

Lysophosphatidic Acid Receptor Type 1 (LPA_1) Plays a Functional Role in Osteoclast Differentiation and Bone Resorption Activity*[S]

Received for publication, November 7, 2013, and in revised form, January 14, 2014 Published, JBC Papers in Press, January 15, 2014, DOI 10.1074/jbc.M113.533232

Marion David[‡1,2,3], Irma Machuca-Gayet[§1], Junichi Kikuta[¶‖], Penelope Ottewell[**], Fuka Mima[¶‖], Raphael Leblanc[‡2], Edith Bonnelye[‡], Johnny Ribeiro[‡], Ingunn Holen[**], Rùben Lopez Vales[‡‡], Pierre Jurdic[§], Jerold Chun[§§], Philippe Clézardin[‡], Masaru Ishii[¶‖], and Olivier Peyruchaud[‡4]

*From the [‡]INSERM, UMR1033, UCB Lyon 1, Faculté de Médecine Lyon Est, 69732 Lyon, France, [§]CNRS, UMR5242, ENS, Équipe Biologie Cellulaire et Physiopathologie Osseuse, Institut de Génomique Fonctionnelle de Lyon, UCB Lyon 1, 69007 Lyon, France, the [¶]Department of Immunology and Cell Biology, Graduate School of Medicine and Frontier Biosciences, Osaka University, 565-0871 Osaka, Japan, [‖]CREST, Japan Science and Technology Agency, 102-0076 Tokyo, Japan, the **Academic Unit of Clinical Oncology, University of Sheffield Medical School, Beech Hill Road, S10 2RX Sheffield, United Kingdom, the [‡‡]Grup de Neuroplasticitat i Regeneració, Unitat de Fisiologia Mèdica, Facultat de Medicina, Universitat Autònoma de Barcelona, 08193 Barcelona, Spain, and the [§§]Department of Molecular Biology, Dorris Neuroscience Center, The Scripps Research Institute, La Jolla, California 92037*

Background: Lysophosphatidic acid (LPA) is a bioactive lipid with pleiotropic activities due to activation of six receptors (LPA_{1-6}).
Results: Genetic deletion and pharmacological blockade of LPA_1 inhibit differentiation and bone degradation activity of osteoclasts.
Conclusion: LPA controls bone homeostasis through the activation of LPA_1 expressed by osteoclasts.
Significance: LPA_1 is a new therapeutic target of diseases with excess bone degradation.

Lysophosphatidic acid (LPA) is a natural bioactive lipid that acts through six different G protein-coupled receptors (LPA_{1-6}) with pleiotropic activities on multiple cell types. We have previously demonstrated that LPA is necessary for successful *in vitro* osteoclastogenesis of bone marrow cells. Bone cells controlling bone remodeling (*i.e.* osteoblasts, osteoclasts, and osteocytes) express LPA_1, but delineating the role of this receptor in bone remodeling is still pending. Despite *Lpar1*$^{-/-}$ mice displaying a low bone mass phenotype, we demonstrated that bone marrow cell-induced osteoclastogenesis was reduced in *Lpar1*$^{-/-}$ mice but not in *Lpar2*$^{-/-}$ and *Lpar3*$^{-/-}$ animals. Expression of LPA_1 was up-regulated during osteoclastogenesis, and LPA_1 antagonists (Ki16425, Debio0719, and VPC12249) inhibited osteoclast differentiation. Blocking LPA_1 activity with Ki16425 inhibited expression of nuclear factor of activated T-cell cytoplasmic 1 (NFATc1) and dendritic cell-specific transmembrane protein and interfered with the fusion but not the proliferation of osteoclast precursors. Similar to wild type osteoclasts treated with Ki16425, mature *Lpar1*$^{-/-}$ osteoclasts had reduced podosome belt and sealing zone resulting in reduced mineralized matrix resorption. Additionally, LPA_1 expression markedly increased in the bone of ovariectomized mice, which was blocked by bisphosphonate treatment. Conversely, systemic treatment with Debio0719 prevented ovariectomy-induced cancellous bone loss. Moreover, intravital multiphoton microscopy revealed that Debio0719 reduced the retention of CX_3CR1-$EGFP^+$ osteoclast precursors in bone by increasing their mobility in the bone marrow cavity. Overall, our results demonstrate that LPA_1 is essential for *in vitro* and *in vivo* osteoclast activities. Therefore, LPA_1 emerges as a new target for the treatment of diseases associated with excess bone loss.

Bone diseases associated with excessive bone loss are among the most prevalent disorders in the population. Hormonal deprivation, inflammation, bone metastasis, and many of the cancer therapeutics alter bone structure, resulting in bone fragility and increased risk of fracture (1). Bone is a complex tissue in which integrity is maintained over the lifetime by the continuous process of bone remodeling supported by specialized bone cells as follows: osteoclasts that resorb bone and osteoblasts that form new bone. Signals emerging from osteocytes (2), immune cells (3), the nervous system (4), as well as hormonal regulation (5) control bone remodeling and modulate crosstalk between osteoclasts and osteoblasts.

Lysophosphatidic acid (LPA)[5] is a natural bioactive phospholipid, exhibiting growth factor-like activities on a range of dif-

* This work was supported by grants from INSERM (to O. P. and P. C.), the Comité Départemental de la Loire de la Ligue Nationale Contre le Cancer (to O. P.), and the French Association pour la Recherche sur le Cancer (to O. P.).
[S] This article contains supplemental Videos 1 and 2.
[1] Both authors contributed equally to this work.
[2] Recipient of a fellowship from the French Association pour la Recherche sur le Cancer.
[3] Recipients of a fellowship from the Ligue Nationale Contre le Cancer.
[4] To whom correspondence should be addressed: INSERM U1033, Faculté de Médecine Lyon Est, Rue Guillaume Paradin, 69372 Lyon Cedex 08, France. Tel.: 33-0478785738; Fax: 33-0478778772; E-mail: olivier.peyruchaud@inserm.fr.

[5] The abbreviations used are: LPA, lysophosphatidic acid; Beta3, integrin beta3; CTR, calcitonin receptor; CTSK, cathepsin K; DC-STAMP, dendritic cell-specific transmembrane protein; FBS, fetal bovine serum; LPA_{1-6}, LPA

ferent cell types, including bone cells (6–9). These activities involve the induction of cytoskeletal rearrangement, cell motility, survival, proliferation, and differentiation (10). Blood platelets are the major source of LPA (11), but we have previously shown that LPA is produced at bone sites in the context of bone metastasis, acting on cancer cells and osteoclasts to promote progression of osteolytic lesions and bone loss (12). More recently, osteoblasts were shown to produce LPA through the involvement of purinergic P2X7 receptor, suggesting that these cells might be an additional source of LPA in bone (13). However, the role of LPA and its cognate receptors *in vivo* on bone cells and bone turnover is not well understood.

The effects of LPA are mediated by at least six different G protein-coupled receptors (LPA$_{1-6}$) (14, 15). These receptors share intracellular signaling pathways dependent on $G\alpha_i$ (LPA$_{1-4}$ and LPA$_6$), $G\alpha_{12/13}$ (LPA$_{1-2}$ and LPA$_{4-6}$), $G\alpha_q$ (LPA$_{1-5}$), and $G\alpha_S$ (LPA$_4$ and LPA$_6$) (16, 17). Therefore, LPA receptors can have potentially redundant or opposite effects on cell biology. Most eukaryotic cells, including bone cells, express numerous LPA receptors. Consequently, pleiotropic activities of LPA are likely dependent on co-activation signals mediated by multiple receptors. As a consequence, activation of different cell types in bone may underlie the complex mode of action of LPA in bone pathophysiology (18).

Lpar1$^{-/-}$ mice have revealed a rich biology and pathophysiology, affecting the brain (19–23) as well as other organ systems like the lung (24), the intestine (25), cardiovascular system (26), the adipose tissue (27), and bone (28). *Lpar2*$^{-/-}$ mice do not exhibit an obvious phenotype (29). In contrast, *Lpar3*$^{-/-}$ female mice are sterile due to defects in embryo implantation (30), and *Lpar3*$^{-/-}$ male mice have age-dependent loss of sperm production (31), indicating a prevalent role of this receptor in the genital tract. *Lpar4*$^{-/-}$ animals showed vascular defects during embryonic development (32) and an osteopetrotic bone phenotype (33). *Lpar5*$^{-/-}$ mice showed reduced susceptibility to pain (34).

LPA plays a key role during bone development as revealed by a low bone mass phenotype of *Lpar1*$^{-/-}$ mice associated with a low osteoblastic activity and growth retardation due to inhibition of chondrocyte proliferation, defects in endochondral ossification (28), and increased bone formation in *Lpar4*$^{-/-}$ animals (33). These reports suggest that LPA$_1$ and LPA$_4$ might have opposite functions in osteoblasts during bone development. In addition to adipogenesis and glucose tolerance defects (27), *Lpar1*$^{-/-}$ mice present developmental abnormalities in the olfactory bulb that markedly impaired pup suckling behavior (19). Deficiencies of the cerebral cortex, food intake, and metabolic regulations are prone to compromise bone homeostasis indirectly. In addition, LPA$_1$ is the most ubiquitous LPA receptor in mammalian tissues (35), expressed in both osteoblasts and osteoclasts (8, 28). Therefore, the bone phenotype of *Lpar1*$^{-/-}$ mice is likely to be a consequence of multiple constraints of bone remodeling involving disruption of both osteoblast and osteoclast activity. Here, we provide the first demonstration that LPA$_1$ controls *in vitro* osteoclast differentiation regulating nuclear factor of activated T-cells cytoplasmic 1 (NFATc1) and dendritic cell-specific transmembrane protein (DC-STAMP) expressions, bone resorption establishing functionally active sealing zone, and *in vivo* controlling motility of osteoclast progenitors in the bone marrow cavity and osteoclast-mediated bone loss induced by ovariectomy.

receptors 1–6; MCSF, macrophage-CSF; NFATc1, nuclear factor of activated T-cells cytoplasmic 1; OVX, ovariectomy; RANK-L, receptor-activated nuclear receptor factor κB ligand; TRAP, tartrate-resistant acid phosphatase; ANOVA, analysis of variance; PTH, parathyroid hormone; EGFP, enhanced GFP; Oc.S, TRAP-positive trabecular bone surface; BS, bone surface.

EXPERIMENTAL PROCEDURES

Drugs and Reagents—Three competitive inhibitors of LPA signaling pathways dependent on LPA$_1$ and LPA$_3$ receptors VPC12249 (Coger, Morillon, France), Ki16425 (Interchim, Montluçon, France), and Debio0719 (generous gift of Dr. Murone, Debiopharm Group, Lausanne, Switzerland) were used (36–38). No antagonist activity of Ki16425 was detected on LPA$_4$, LPA$_5$, and LPA$_6$ (37, 39, 40). No data are currently available supporting antagonist activities of Debio0719 and VPC12249 on these receptors. Zoledronic acid was obtained from Novartis (Basel, Switzerland). Risedronate was obtained from Procter & Gamble Pharmaceuticals (Cincinnati, OH).

Animal Studies—Mice used at the Université Claude Bernard Lyon1 (Lyon, France) were handled according to the rules of Décret Number 87-848 of October 19, 1987, Paris. The experimental protocol have been reviewed and approved by the Institutional Animal Care and Use Committee of the Université Claude Bernard Lyon-1 (Lyon, France). Animal experiments performed at the University of Sheffield were carried out in accordance with local guidelines and with home office approval under Project License 40/3531, University of Sheffield (Sheffield, UK). Animal experiments carried out at the University of Osaka were performed according to National Institutes of Health institutional guidelines and Osaka University animal experimental guidelines under approved protocols. Studies were routinely inspected by the attending veterinarian to ensure continued compliance with the proposed protocols. Mice were maintained on a 12:12-h light/dark cycle, and autoclaved water and mouse chow were provided ad libitum. *Lpar1*$^{-/-}$- and *Lpar3*$^{-/-}$-deficient mice originally generated in a C57Bl/6 background were backcrossed more than 12 times with BALB/c females (19, 30). *Lpar2*$^{-/-}$ knock-out mice generated in a C57BL/6–129/SvJ background were described previously (29). Animals were genotyped by PCR following the procedures described previously (19, 29, 30). CX$_3$CR1-GFP knock-in mice (41) were obtained from The Jackson Laboratory. Mutant mice were genotyped by PCR. BALB/c mice were obtained from Janvier SA (Le Genest St. Isle, France). Female BALB/c nude mice were obtained from Charles River (Kent, UK).

Ovariectomy—Nine-week-old female BALB/c mice were anesthetized by intraperitoneal injection of a xylazine (0.1%, w/v)/ketamine (0.75%) mixture. After dorsal incision of the abdominal wall, the ovaries were picked clean from the surrounding fat tissue and removed (ovariectomy) or replaced without injury (sham-operated mice). Animals were subjected to daily intraperitoneal injections of risedronate (5 mg/kg) or twice daily per os injection of Debio0719 (50 mg/kg) or vehicle

(saline). Mice were euthanized 30 days after OVX. To confirm the efficiency of OVX, uteri were removed and weighed at the end of the experiments. Bones from all euthanized mice were dissected out and used either for μCT imaging or histological analysis. Total RNA extraction from bone was carried out on 12-week-old female BALB/c nude mice (Charles River, Kent, UK). On day 0, 18 mice per group were injected with 100 μg/kg zoledronic acid or 0.1 ml of saline intraperitoneally. Three days after injection, nine mice from each group were either ovariectomized or sham-operated before sacrifice on day 10. Tibiae and femurs from three mice per group were pooled and flash-frozen in liquid nitrogen.

Two-photon Intravital Bone Tissue Imaging—CX$_3$CR1-EGFP mice were subcutaneously administered either Debio0719 (20 mg/kg body weight) or vehicle (DMSO in PBS). Four hours after administration, bone tissues of these mice were visualized to measure the mobility of EGFP$^+$ cells by intravital microscopy. Experiments were carried out on mouse calvaria bone tissues using a protocol modified from a previous study (42). Mice were anesthetized with isoflurane (Escain; 2.0% (v/v) vaporized in 100% (v/v) oxygen), and hair at the neck and scalp was removed with hair removal lotion (Epilat). The frontoparietal skull was exposed, and the mouse head was immobilized in a custom-made stereotactic holder. The imaging system was composed of a multiphoton microscope (A1-MP; Nikon) driven by a laser (Chameleon Vision II Ti: Sapphire; Coherent) tuned to 880 nm and an upright microscope (APO, N.A. 1.1; Nikon) equipped with a 25× water immersion objective (HCX APO, N.A. 1.0; Leica). The microscope was enclosed in an environmental chamber in which anesthetized mice were warmed by heated air. Fluorescent cells were detected through a bandpass emission filter at 525/50 nm (for EGFP). Vessels were visualized by injecting 70 kDa of Texas red-conjugated dextran (detected using a 629/56 nm filter) i.v. immediately before imaging. Image stacks were collected at a 5-μm vertical step size at a depth of 100–150 μm below the skull bone surface. The time resolution was 1 min. Raw imaging data were processed with Imaris (Bitplane) with a Gaussian filter for noise reduction. Automatic three-dimensional object tracking with Imaris Spots was aided with manual corrections to retrieve cell spatial coordinates over time.

Three-dimensional μCT—Microcomputed tomography analyses were carried out using a μCT scanner Skyscan 1174 (Skyscan; Kontich, Belgium). The x-ray tube was set to a voltage of 50 kV and a current of 800 mA. A 0.5-mm aluminum filter was used to reduce beam-hardening artifacts. Samples were scanned in 70% ethanol with a voxel size of 10.3 μm. For each sample, 265 section images were reconstructed with NRecon software (version 1.6.1.8, Skyscan). Three-dimensional modeling and analysis of bone volume/trabecular volume, were obtained with the CTAn (version 1.9, Skyscan) and CTVol (version 2.0, Skyscan) software. The dissected bones were then processed for histological analysis.

Bone Histology—Hind limbs were fixed, decalcified with 16% EDTA, and embedded in paraffin. Five-μm tissue sections were stained with Goldner's Trichrome and processed for histomorphometric analysis. *In situ* detection of osteoclasts was carried out on tissue sections using the tartrate-resistant acid phosphatase (TRAP) activity kit assay (Sigma). The resorption surface (Oc.S/BS) was calculated as the ratio of TRAP-positive trabecular bone surface (Oc.S) to the total trabecular bone surface (BS) using the computerized image analysis system Morpho-Expert (Exploranova).

Osteoclastogenesis Assay—Bone marrow cells from hind limbs of 6-week-old male mice were collected and seeded in 12-well tissue culture plates at a density of 2×10^5 cells per well in α-minimal essential medium (Invitrogen) supplemented with 10% v/v FBS (Life Technology, Saint Aubain, France), 1% penicillin/streptomycin (Life Technology), 1% L-glutamine (Sigma), 25 ng/ml macrophage-CSF (R&D Systems, Lille, France), 100 ng/ml receptor-activated nuclear receptor factor κB ligand (RANK-L). Culture media were then supplemented with or without Ki16425 (10 μM), Debio0719 (1 μM), or VPC12249 (10 μM). After 6 days, mature osteoclasts were enumerated under a microscope on the basis of the number of nuclei ($n \geq 3$) and the TRAP activity (Sigma). Results were expressed as the number of osteoclasts per well.

Podosome Belt and Sealing Zone Quantification—Osteoclasts in culture on glass coverslips were fixed in 4% paraformaldehyde, pH 7.2, for 10 min, permeabilized with 0.2% Triton X-100 in PBS for 5 min, then saturated with 2% BSA in PBS, followed by incubation with rhodamine-conjugated phalloidin to reveal F-actin. Osteoclasts in culture on bovine cortical bone slices were fixed with 4% paraformaldehyde in PBS for 10 min at 37 °C and permeabilized using PBS + 0.2% Triton X-100 in PBS. Then cells were incubated for 20 min with Alexa Fluor® 488 phalloidin (Invitrogen) diluted 1:100. Image acquisition was performed with an inverted confocal microscope Zeiss LSM780 using GaAsP PMT and an EC-Plan-Neofluar 20×/0.5 objective. The surface area was measured manually with ImageJ software.

Resorption Assay—Osteoclast efficacy to resorb mineralized matrix was carried out using apatite collagen complex (Corning Glass). Two hundred osteoclasts of each genotype were plated in each well and left to resorb for 48 h. Cells were removed by a gentle shaking in 0.001% Triton buffer lysis for 1 h; the matrix was stained with silver nitrate, and the resorption pits were detected under a light microscope. To measure the resorbed surface area, a series of 99 micrographs were imaged using a DMI system, and the mosaic of each well was reconstituted using a plugin of ImageJ software. The pit surface per single osteoclast was quantified with ImageJ, and data were reported as resorbed mineralized surfaces in μm^2/Oc. Alternatively, an equivalent number of pre-osteoclasts isolated from WT BALB/c mice were cultured for 4 days. Then the culture media was supplemented with Ki16425 (10 μM) for an additional 3 days. The culture was then stopped, and pit surfaces were determined as described above.

Reverse Transcription and RT-PCR—Total RNAs from osteoclast cultures were extracted using Nucleospin RNAII kit (Macherey-Nagel, Hoerdt, France) and from powdered whole bone with TRIzol (Invitrogen). Complementary DNA from osteoclasts and bones were synthesized by reverse transcription using iScript cDNA synthesis kit (Bio-Rad) and Superscript III (Invitrogen), respectively. Expression of target genes was quantified by real time quantitative RT-PCR on an Eppendorf Mas-

TABLE 1
List of specific primer sets
F is forward, and R is reverse.

Name	Sequence 5′–3′	°C	Slope	Intercept
LPA1-F	CCAGGAGGAATCGGGACAC	63	−3.48	20.52
LPA1-R	CAATAACAAGACCAATCCCGGA			
LPA2-F	GTCAAGACGGTTGTCATCATTCT	67	−3.27	25.07
LPA2-R	GAAGCATGATCCGCGTGCT			
LPA3-F	ACAAAGCTTGTGATCGTCCTGT	63	−3.223	22.78
LPA3-R	TCATGATGGACATGTGTGTTTCC			
LPA4-F	GCATTGTTGACATTAGTGGTGGA	63	−3.256	26.46
LPA4-R	AACCTGGCCCTCTCTGATTT			
LPA5-F	CCGTACATGTTCATCTGGAAGAT	63	−3.747	24.60
LPA5-R	CAGACTAATTTCTCTTCCCACCT			
LPA6-F	TGTTTCCAACTGCTGCTTTG	58	−3.535	22.75
LPA6-R	GAGCAGTCCCAGTGGCTTAG			
Beta-3-F	GATGACATCGAGCAGGTGAAAGAG	67	−3.137	21.42
Beta-3-R	CCGGTCATGAATGGTGATGAGTAG			
CTR-F	AGCCACAGCCTATCAGCACT	67	−3.546	17.52
CTR-R	GTCACCCTCTGGCAGCTAAG			
CTSK-F	GAGGGCCAACTCAAGAAGAA	65	−2.972	18.89
CTSK-R	GCCGTGGCGTTATACATACA			
ATP6v0D2-F	TCAGATCTCTTCAAGGCTGTGCTG	67	−3.718	17.52
ATP6v0D2-R	GTGCCAAATGAGTTCAGAGTGATG			
cFMS-F	AACATATGGACTTCGCCCTC	65	−3.34	13.20
cFMS -R	CTAGCACTGTGAGAACCCCA			
NFATc1-F	GGTCTTCCGAGTTCACATCC	60	−3.595	14.38
NFATc1-R	GCCTTCTCCACGAAAATGAC			
c-Fos-F	CCGCATGGAGTGTGTTGTTCC	67	−3.594	14.10
c-Fos-R	GACCACCTCGACAATGCATGA			
DC-STAMP-F	GGGCACCAGTATTTTCCTGA	60	−3.644	16.04
DC-STAMP-R	CAGAACGGCCAGAAGAATGA			
L32-F	CAAGGAGCTGGAGGTGCTGC	60	−4.071	12.61
L32-R	CTGCTCTTTCTACAATGGC			

tercycler® RealPlex (Eppendorf, Sartrouville, France) using the SYBR® Green PCR kit (VWR International, Fontenay-Sous-Bois, France) and sets of specific primers (Table 1). Quantifications were normalized to corresponding RNA *L32* values and expressed as relative expression using the $2(-\Delta\Delta C_T)$ method (43).

Statistical Analysis—Differences between groups were determined by one- or two-way ANOVA followed by Bonferroni post-test using GraphPad Prism Version 5.0c software. Single comparisons were carried out using two-sided unpaired *t* test. $p < 0.05$ was considered significant.

RESULTS

Expression of LPA Receptors during Osteoclastogenesis—Osteoclastogenesis depends on a sequential gene activation program controlling the proliferation of osteoclast precursors that successively fuse to form large polykaryons that eventually differentiate into fully active multinucleated osteoclasts (44). Primary culture of bone marrow cells (BMCs) extracted from WT BALB/c mice in the presence of MCSF and RANK-L was performed. In agreement with previous reports showing high expression levels of LPA_6(P2Y5) in hematopoietic cells and during monocyte-to-macrophage differentiation (45), we found by real time PCR (Fig. 1*A*) that LPA_6 had the highest expression levels in BMCs (data not shown) and at day 1 of osteoclastogenesis that decreased to high and stable values from days 2 to 5. LPA_3 was not detected in osteoclast progenitors and during osteoclastogenesis, whereas LPA_1 expression prevailed among all other LPA receptors at both early (days 1–3) and late (days 3–5) stages of osteoclast differentiation. Also, LPA_1, LPA_2, LPA_4, and LPA_5 were up-regulated from days 3 to 4 concomitantly with the expression of osteoclast differentiation markers (ATP6v0d2, integrin β3 (Beta3), calcitonin receptor (CTR), and cathepsin K (CTSK)) (Fig. 1*B*). These data suggest that LPA_1 and LPA_6 potentially regulate the behavior of both osteoclast precursors and mature osteoclasts, whereas the activity of other LPA receptors might only play a role during the latter stages of osteoclast differentiation.

Inhibiting LPA$_1$ Activity Impairs Osteoclastogenesis—To determine the role of LPA receptors in osteoclastogenesis, primary cultures of BMCs collected from *Lpar1*$^{-/-}$, *Lpar2*$^{-/-}$, and *Lpar3*$^{-/-}$ mice and WT littermates were performed in the presence of MCSF and RANK-L. After 6 days, we found that the number of tartrate-resistant acid phosphatase (TRAP)-positive multinucleated cells (mature osteoclasts) from *Lpar1*$^{-/-}$ mice was significantly lower by 62% to that obtained with WT cells (316 ± 82.2 and 831 ± 78.6, $p < 0.001$) (Fig. 1, *C* and *D*). In marked contrast, the numbers of mature osteoclasts generated from *Lpar2*$^{-/-}$ and *Lpar3*$^{-/-}$ mice were identical to those obtained from WT cells with matched genetic background (Fig. 1, *C* and *D*). Inhibition of osteoclast differentiation in *Lpar1*$^{-/-}$ cells was confirmed at the transcriptomic level, because the expression of osteoclast markers was markedly decreased compared with WT cells (Fig. 1*E*). Altogether these results suggest the implication of LPA_1 in osteoclast differentiation, although LPA_2 or LPA_3 appear not to be involved. Hematopoietic osteoclast precursors, monocytes, do not express LPA_3 (46, 47). Because our previous observations showed no LPA_3 expression at all stages of osteoclastogenesis (Fig. 1*A*), we next considered cells from the osteoclast lineage as LPA_3-null cells. Thus, to further investigate the role of LPA_1 in osteoclast differentiation, we decided to use a pharmacological approach to inhibit LPA_1 activity. We treated BMC precursors with nonspecific LPA_1/

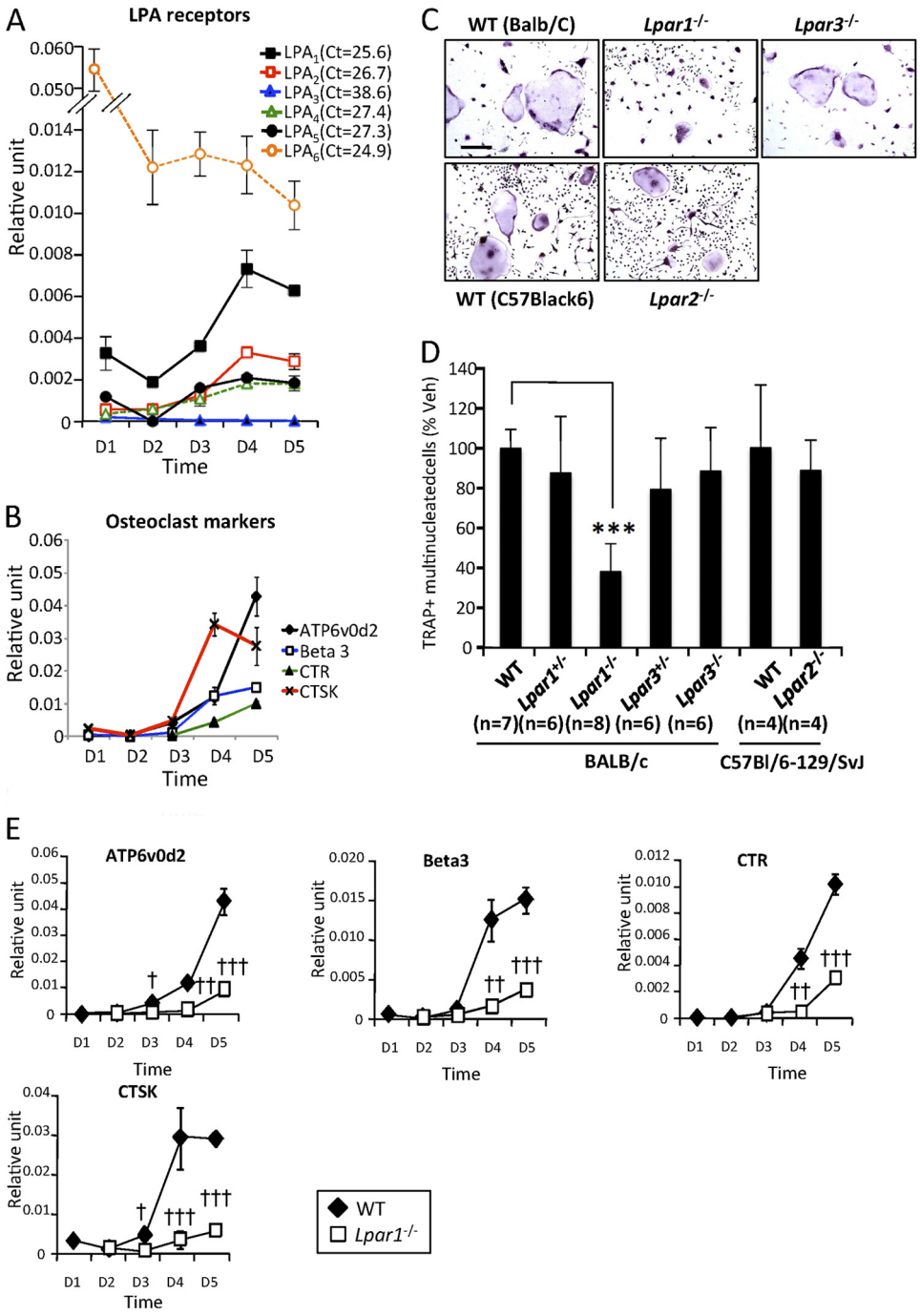

FIGURE 1. **Impaired osteoclast differentiation in culture of *Lpar1*$^{-/-}$ but not *Lpar2*$^{-/-}$ and *Lpar3*$^{-/-}$ bone marrow cells.** *A,* time course of expression of LPA receptors (LPA$_{1-6}$); *B,* ATP6v0d2, Beta3, CTR, and CTSK mRNA in bone marrow cell from wild type BALB/c mice cultured with serum + MCSF + RANK-L. Values were normalized to housekeeping *L32* gene. All values were the mean ± S.D. of three experiments. *C,* micrographs of bone marrow cells from LPA receptor mutants (−/−), heterozygous (+/−), and wild type (*WT*) mice from BALB/c and C57Bl/6–129/SvJ backgrounds, grown with serum + MCSF + RANK-L and stained for TRAP activity (*TRAP*$^+$). *D,* number of TRAP$^+$ multinucleated cells per well. All values are the mean ± S.D. of 4–8 experiments. ***, $p < 0.001$ *versus* WT BALB/c bone marrow cells using one-way ANOVA with a Bonferroni post-test. *Bar scale* represents 100 μm. *veh,* vehicle. *E,* time course of expression of ATP6v0d2, Beta3, CTR, and CTSK mRNA in bone marrow cells from wild type BALB/c (*open symbols*) and *Lpar1*$^{-/-}$ mice cultured with serum + MCSF + RANK-L. Values were normalized to housekeeping *L32* gene. All values were the mean ± S.D. of three experiments. †, $p < 0.05$; ††, $p < 0.01$; †††, $p < 0.001$; *versus* wild type cells using two-way ANOVA with a Bonferroni post-test. *D,* day.

LPA$_3$ antagonists (Ki16425, Debio0719, and VPC12249). Each LPA$_1$ inhibitor reduced MCSF/RANK-L-induced osteoclastogenesis of WT BMC precursors by 55% (VPC12249), 68% (Ki16425), or 83% (Debio0719) (Fig. 2*A*). Interestingly, the extent of inhibition caused by LPA$_1$ antagonists was not statistically significantly different to that observed with *Lpar1*$^{-/-}$ BMCs (62%) (Fig. 2*A*). As presented above (Fig. 1*A*), LPA$_2$ was also up-regulated during osteoclastogenesis; therefore, we investigated whether blocking of both LPA$_1$ and LPA$_2$ activity would inhibit osteoclastogenesis to a further extent. We found that supplementing *Lpar2*$^{-/-}$ BMC culture media with Ki16425 inhibited the differentiation of osteoclasts by 62% (Fig. 2*B*), which was

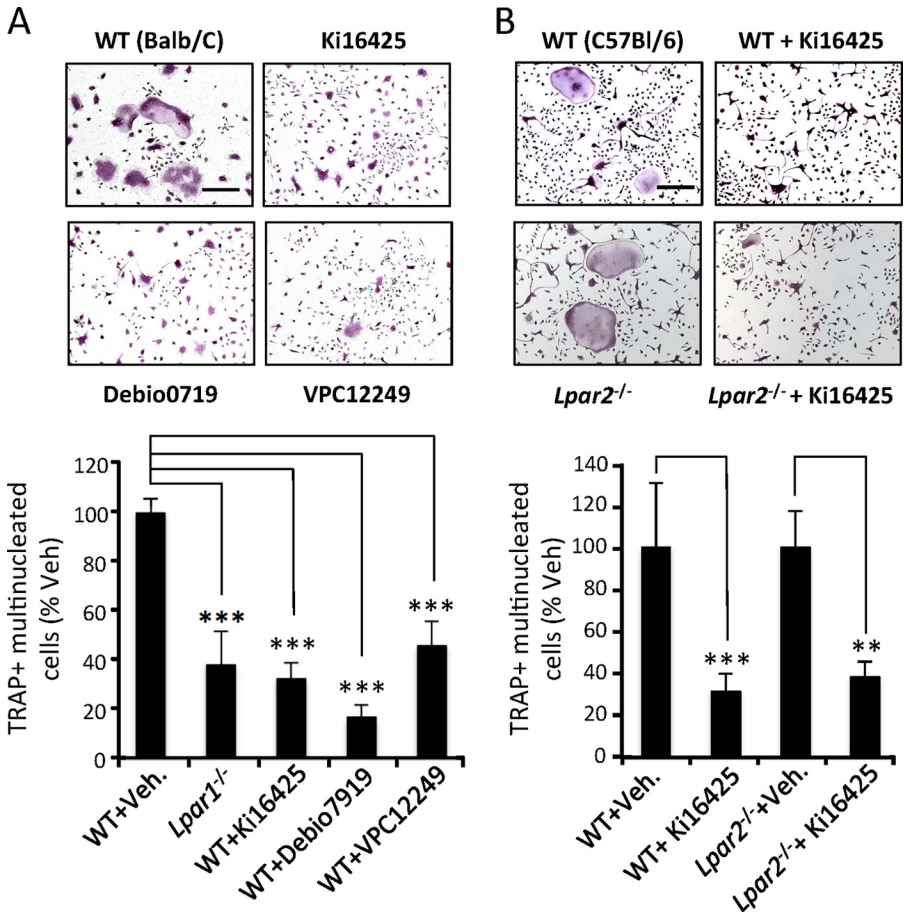

FIGURE 2. **Antagonists of LPA$_1$ impair osteoclast differentiation from primary culture bone marrow cell culture.** *A,* visualization of TRAP$^+$ multinucleated osteoclasts obtained from wild type BALB/c mice grown with serum + MCSF + RANK-L in the presence of vehicle (*WT+Veh*) or Ki16425 (10 μM), Denio0719 (1 μM), or VCP12249 (10 μM) (*upper panels*) and evaluation of number of TRAP$^+$ multinucleated cells in % of vehicle-treated cells (*lower panel*). *B,* micrographs of bone marrow cells from wild type C57Bl/6–129/SvJ (C57Bl/6) or *Lpar2*$^{-/-}$ mice grown with serum + MCSF + RANK-L in the presence of vehicle (*WT*) or Ki16425 (10 μM) and stained for TRAP activity (*upper panels*). Number of TRAP$^+$ multinucleated cells in % of vehicle-treated cells (*lower panel*). All values are the mean ± S.D. of 3 to 4 experiments. **, $p < 0.01$; ***, $p < 0.001$ *versus* vehicle-treated cells with the same genotype using one-way ANOVA with Bonferroni post-test. *Bar scales,* 100 μm.

not significantly different from the inhibition of osteoclast formation caused by Ki16425 treatment of WT BMCs (69%, Fig. 2*A*). This result indicates that blocking of both LPA$_1$ and LPA$_2$ activity does not inhibit osteoclastogenesis to a greater extent than that achieved by blocking LPA$_1$ alone.

We next investigated whether LPA$_1$ plays a role in a particular phase of osteoclastogenesis (proliferation, fusion, and differentiation). We found that a short treatment period with Ki16425 during the proliferation phase of osteoclast precursors (days 1–3 and days 2 and 3), or during the late phase of mature osteoclast differentiation (days 5–7), did not significantly affect the final number of osteoclasts (Fig. 3, *A* and *B*). In contrast, when added during the fusion phase of osteoclast precursors (days 3–4, 3–5, and 4–5), Ki16425 significantly inhibited the formation of osteoclasts by 48% at days 3–5 ($p < 0.001$) and days 4 and 5 ($p < 0.001$) and by 58% at days 3 and 4 ($p < 0.001$)) compared with vehicle-treated BMCs (Fig. 3, *A* and *B*). Additionally, the levels of inhibition were not statistically significantly different from the 69% inhibition of osteoclastogenesis resulting from addition of Ki16425 from days 1 to 7. When added between days 3 and 5, Ki16425 also significantly induced an accumulation of osteoclasts with a low number of nuclei ($3 \leq n < 5$) compared with vehicle-treated cells (73 *versus* 40%; $p < 0.05$) and a decrease in the number of osteoclasts with a high number of nuclei; $5 \leq n < 10$ and $n > 10$ (25% *versus* 50%; $p < 0.001$) and (2% *versus* 10%; $p < 0.05$), respectively. Also, a significant accumulation by 69% ($p < 0.05$) of osteoclasts with low number of nuclei ($3 \leq n < 5$) was observed in *Lpar1*$^{-/-}$ BMC cultures. Altogether, these results indicated that blocking LPA$_1$ activity inhibited the fusion of osteoclast precursors (Fig. 3*C*). In agreement with previous observations on *Lpar1*$^{-/-}$ BMCs, inhibiting LPA$_1$ activity with Ki16425 significantly decreased the expression of markers of osteoclast activity (ATP6v0d2, CTR, Beta3, and CTSK) (Fig. 3*D*). In addition, compared with vehicle, Ki16425 had no effect on the expression of LPA$_1$, the transcription factor c-Fos, and the MCSF receptor cFMS that are expressed at the early stage of osteoclast differentiation, whereas expressions of the pro-survival NFATc1 and the fusion protein DC-STAMP that are implicated in fusion and differentiation were significantly decreased by 50% ($p = 0.003$) and 70% ($p = 0.021$), respectively (Fig. 3*D*).

Inhibiting LPA$_1$ Activity Impairs the Cytoskeletal Organization in Mature Osteoclasts—Osteoclastic bone resorption activity is dependent on a highly specialized organization of the

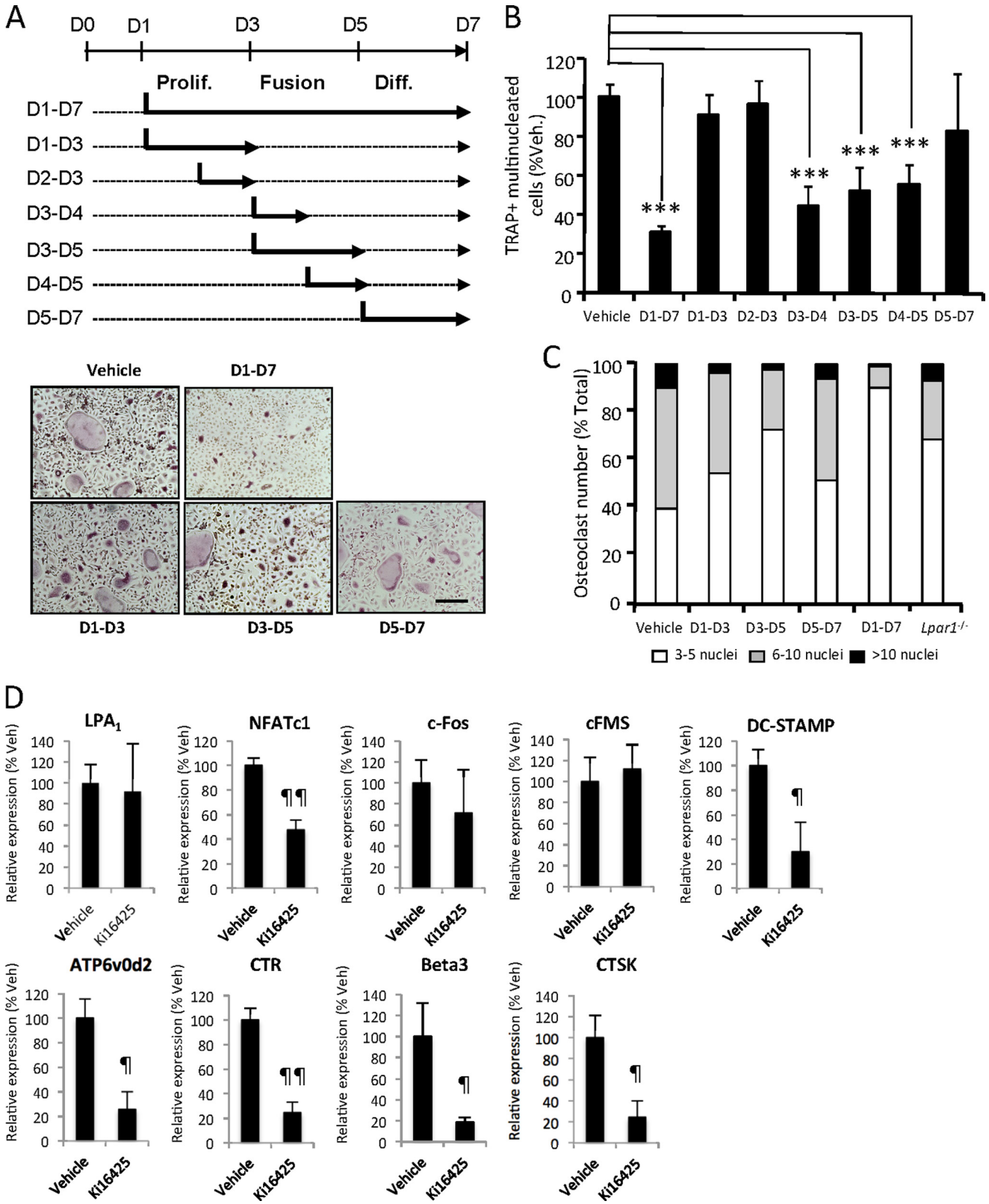

FIGURE 3. **Inhibition of LPA$_1$ activity impairs osteoclast fusion.** *A,* schematic representation of treatment schedule of bone marrow cells from wild type BALB/c mice grown with serum + MCSF + RANK-L in the absence (*dotted lines*) or presence of Ki16425 (*bold lines*) (*upper panel*). Micrographs of cells stained for TRAP activity (*lower panels*). *Prolif,* proliferation; *Diff,* differentiation. *B,* number of TRAP$^+$ multinucleated cells in % of vehicle-treated cells. ***, $p < 0.001$ *versus* vehicle-treated cells using one-way ANOVA with Bonferroni post-test. *C,* repartition of osteoclasts number in Ki16425- *versus* vehicle-treated cells with Ki16425 according to the number of nuclei. *D,* real time PCR analysis of LPA$_1$, NFATc1, c-Fos, c-Fms, DC-STAMP, ATP6v0d2, CTR, Beta3, and CTSK mRNA expression in bone marrow cells cultured for 6 days in presence of vehicle (*Veh*) or Ki16425. Values are normalized to housekeeping gene *L32*. All values are the mean ± S.D. of three experiments. ¶, $p < 0.05$; ¶¶, $p < 0.01$ *versus* wild type osteoclasts using two-sided unpaired *t* test. *Bar scale,* 100 μm. *D,* day.

actin cytoskeleton (48). Because induction of cytoskeletal rearrangements is a hallmark of LPA activity (49), we investigated the role of LPA_1 in osteoclast actin cytoskeleton organization. Mature osteoclasts from BMCs of *Lpar1*$^{-/-}$ and WT animals were generated on glass coverslips and stained with rhodamine-phalloidin. The number of osteoclasts with a complete podosome belt was determined by epifluorescence microscopy. We found that the proportion of *Lpar1*$^{-/-}$ osteoclasts with a complete podosome belt was significantly lower than that of WT osteoclasts (35% *versus* 58%; $p < 0.001$) (Fig. 4*A*). This experiment was repeated with WT cells seeded on bovine cortical bone slices. Under these conditions, osteoclasts form a complex podosome belt-like structure rich in F-actin named the sealing zone, which is required for successful osteoclastic bone resorption (48). We observed that within 30 min, Ki16425 (10 μM) reduced the percentage of osteoclasts with detectable sealing zone by 48.6% as a consequence of a decrease in the percentage of osteoclasts with both complete (8% *versus* 25.6%; $p < 0.001$) and discontinued sealing zones (48% *versus* 74.4%; $p < 0.05$) (Fig. 4*B*). Moreover, Ki16425 decreased the area covered by the sealing zone in each osteoclast by 40.2% (Fig. 4*B*). These results suggest that inhibition of LPA_1 activity might reduce the capacity of osteoclasts to adhere to the bone matrix, impairing the formation of a fully efficient sealing zone and hence inhibit bone resorption.

Inhibiting LPA$_1$ Activity Impairs Osteoclast Bone Resorption Activity—To analyze the role of LPA_1 in osteoclast bone resorption activity, we first generated WT and *Lpar1*$^{-/-}$ osteoclasts from BMCs on conventional culture plates, detached the multinucleated cells, and seeded the same number of osteoclasts on mineralized tissue culture plates (apatite collagen complex). We then imaged and quantified the resulting lacunae by phase contrast microscopy. The mean resorbed mineral surfaces generated by *Lpar1*$^{-/-}$ osteoclasts was significantly lower compared with that of WT osteoclasts (1190 $\pm$ 222 μm^2 *versus* 329 $\pm$ 81 μm^2; $p = 0.0013$) (Fig. 5*A*). Treatment of WT osteoclasts with Ki16425 (10 μM) reduced the mean resorbed mineral surface area by 60% (2413 $\pm$ 402 μm^2 *versus* 946 $\pm$ 118 μm^2; $p = 0.005$) (Fig. 5*B*). Additionally, 72 h of treatment of mature WT osteoclasts generated on dentin slices with Ki16425 caused a 26% decrease in the density of osteoclasts (542 $\pm$ 23.1 *versus* 400 $\pm$ 31.8 per cm^2; $p = 0.01$) with noticeable overspreading of Ki16425-treated osteoclasts attached to the dentin (Fig. 5*C*). These results indicate that LPA_1 is essential for optimal bone resorption and that blocking LPA_1 activity might reduce the tight adhesion of osteoclasts to the mineralized matrix required for resorption activity.

Inhibition of LPA$_1$ Activity Prevents Osteoclast-induced Cancellous Bone Loss—Decreased levels of estrogen are responsible for osteoporosis mediated by increased osteoclast activation and excessive bone loss in postmenopausal women. Osteoporosis can be mimicked in animals by OVX (50). Four weeks after surgical intervention, we collected distal femur and tibia metaphyses of ovariectomized and sham mice, extracted total bone RNAs, and measured expression of LPA receptors by RT-quantitative PCR. Expression of LPA_6 was predominant in the bone of sham-operated mice, whereas LPA_1, LPA_3, PLA_4, and LPA_5 were found at lower levels, and LPA_2 was barely detectable

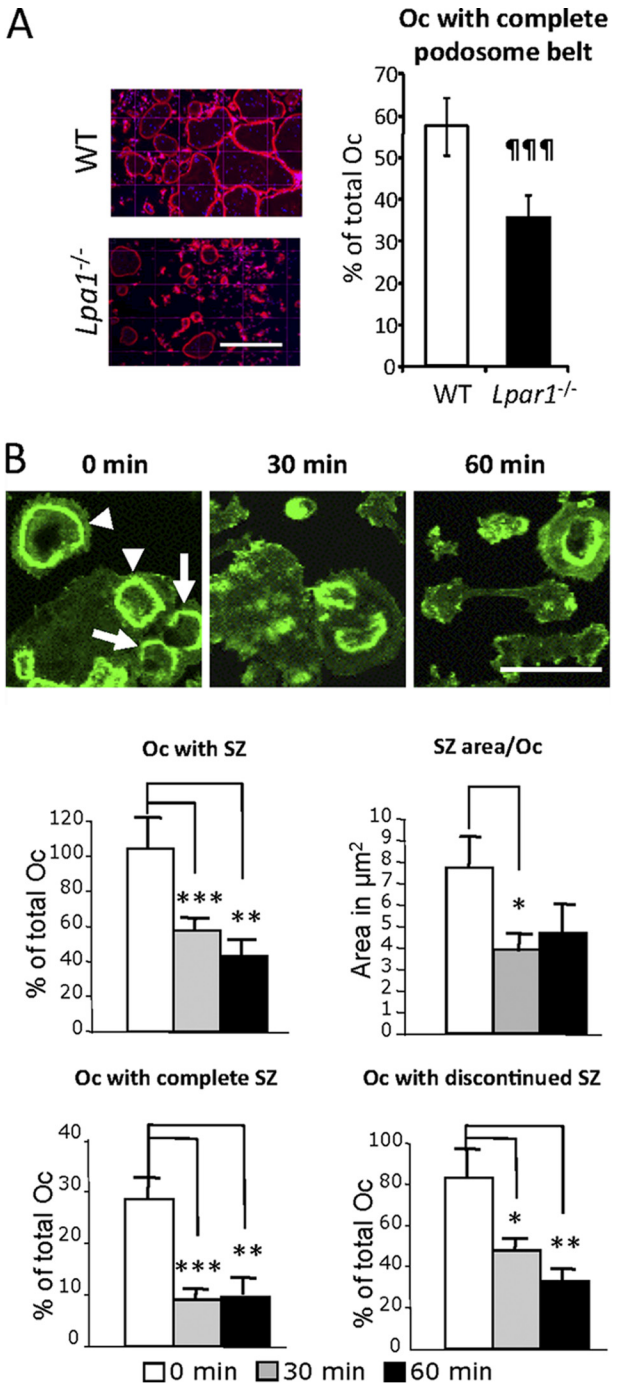

FIGURE 4. **Blocking LPA_1 activity interferes with podosome belt and sealing zone organizations.** *A,* micrographs of mature osteoclasts (*Oc*) from *Lpar1*$^{-/-}$ and wild type (*WT*) mice seeded on glass coverslips and stained with rhodamine-conjugated phalloidin (*left panels*). Percentage of osteoclasts with complete podosome belts (*right panels*) *Bar scale,* 200 μm. ¶¶¶, $p < 0.001$ *versus* wild type osteoclasts using two-sided unpaired *t* test. *B,* micrographs of mature osteoclasts from wild type mice seeded on bone slices and incubated with Ki16425 (10 μM) for 0, 30, and 60 min and stained with Alexa Fluor® 488 phalloidin (*upper panels*). Percentage of osteoclasts with sealing zones (*SZ*), with complete sealing zone, and with discontinued sealing zone, and area of sealing zone per osteoclast (*lower panels*). *, $p < 0.05$; **, $p < 0.01$, ***, $p < 0.001$ *versus* 0-min-treated cells using one-way ANOVA with Bonferroni post-test. *Arrowheads* indicate osteoclasts with a complete sealing zone. *Arrows* indicate osteoclasts with discontinued sealing zones. *Bar scale,* 100 μm.

(Fig. 6). Following OVX, the expression of LPA_6 was not significantly modified, whereas LPA_1 was dramatically increased ($\times$11.3-fold) and LPA_4 to a lesser extent ($\times$1.7-fold), although

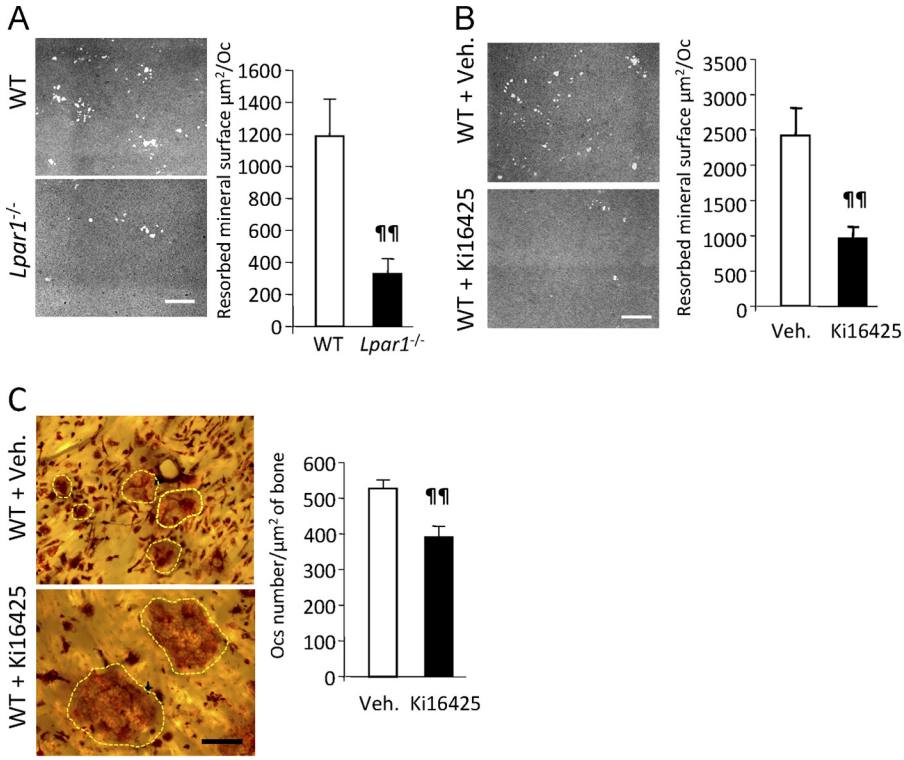

FIGURE 5. **Blocking LPA$_1$ activity inhibits osteoclast resorption.** *A,* micrographs of mineralized matrix apatite collagen complex incubated for 48 h with mature osteoclasts from *Lpar1*$^{-/-}$ or wild type (*WT*) mice (*left panels*). Resorbed mineral surface areas are shown in the *right panes*. ¶¶, $p < 0.01$ *versus* wild type osteoclasts using two-sided unpaired *t* test. *B,* micrographs of mineralized matrix apatite collagen complex incubated for 48 h with mature osteoclasts from wild type mice in the presence or absence Ki16425 (10 μM) (*left panels*). Resorbed mineral surface areas are shown in the *right panel*. ¶¶, $p < 0.01$ *versus* vehicle-treated cells using two-sided unpaired *t* test. *C,* micrographs of TRAP-stained osteoclasts differentiated on bone slices treated with vehicle or Ki16425 from days 4 to 7 (*left panels*). Osteoclasts were highlighted with *yellow dotted lines*. Osteoclast numbers per μm^2 of bone slice in the presence or absence of Ki16425 are shown in the *right panel*. ¶¶, $p < 0.01$ *versus* vehicle (*veh*)-treated cells using two-sided unpaired *t* test. *Bar scales,* 100 μm in *A* and *B* and 50 μm in *C*.

other receptors were down-regulated compared with sham-operated animals: LPA_3 (×7.1-fold) and LPA_5 (×35.5-fold) (Fig. 6*A*). As expected, osteoclast activation markers (CTR and CTSK) were up-regulated in bone following OVX due in part to an increase in osteoclast differentiation (Fig. 6*B*). Remarkably, along with reducing the expression of osteoclast markers, the anti-resorptive agent zoledronic acid inhibited up-regulation of LPA_1 in the bone of ovariectomized animals (Fig. 6*B*). These results indicate that increased osteoclastic bone resorption *in vivo* is associated with up-regulation of LPA_1.

We next investigated the contribution of LPA_1 during the process of hyper-resorptive bone loss *in vivo*. Nine-week-old female mice were ovariectomized and treated daily for 4 weeks with vehicle or the Ki16425 structurally related LPA_1 antagonist Debio0719 (20 mg/kg) (38) or the anti-resorptive agent risedronate (4 mg/kg). We used μCT imaging analyses of the distal femurs to assess histomorphometric parameters of the trabecular bone. As expected, risedronate treatment inhibited trabecular bone loss, resulting in a bone volume/trabecular volume value not significantly different from that of sham-operated animals (23% ± 2.0 *versus* 26% ± 3.5) (Fig. 7*A*). Although the bone volume/trabecular volume value in animals treated with Debio0719 was lower than in sham mice, it was significantly higher than in OVX animals treated with vehicle (19% ± 3.1 *versus* 14% ± 4.1; $p < 0.05$) (Fig. 7, *A* and *B*). Overall, these data indicate that systemic treatment of animals with the LPA_1 antagonist Debio0719 prevented by 60% trabecular bone loss induced by OVX.

Serum bone resorption markers are known to gradually increase during the first 2 weeks following OVX and then rapidly return to base line the week after (51). Therefore, 4 weeks after OVX, osteoclast activity in the bone of animals treated with Debio0719 was analyzed by histological examinations of tissue sections of tibia epiphyses stained for TRAP activity. As expected, risedronate treatment completely blocked the OVX-induced increase in osteoclast number (Oc.S/BS) (Fig. 7*B*). There was no significant difference in Oc.S/BS ratio in animals treated with Debio0719 compared with the sham group (28.2 ± 4.5% *versus* 28.7 ± 4.8%). Altogether, these results indicate that systemic treatment with Debio0719 inhibited bone resorption through a mechanism involving impairment of the differentiation and/or the recruitment of osteoclast precursors at the bone surface.

Inhibiting LPA$_1$ Activity Impairs the Dynamic Behavior of Circulating Osteoclast Precursors—To investigate the role of LPA_1 on osteoclast precursor migration *in vivo*, we performed intravital two-photon imaging of calvaria from CX_3CR1-$EGFP^+$ mice, examining the migratory behavior of fluorescent monocytoid cells containing osteoclast precursors resident in the marrow spaces. First, we measured the expression of mRNAs encoding different LPA receptors in CX_3CR1^+ osteoclast precursor monocytes. CX_3CR1^+ cells from BMCs were collected using a cell sorter and analyzed by RT-PCR. In agreement with the results presented above, we found that LPA_1, LPA_2, LPA_4, LPA_5, and LPA_6 were expressed in CX_3CR1^+ osteoclast precursors, whereas LPA_3 expression was not detectable

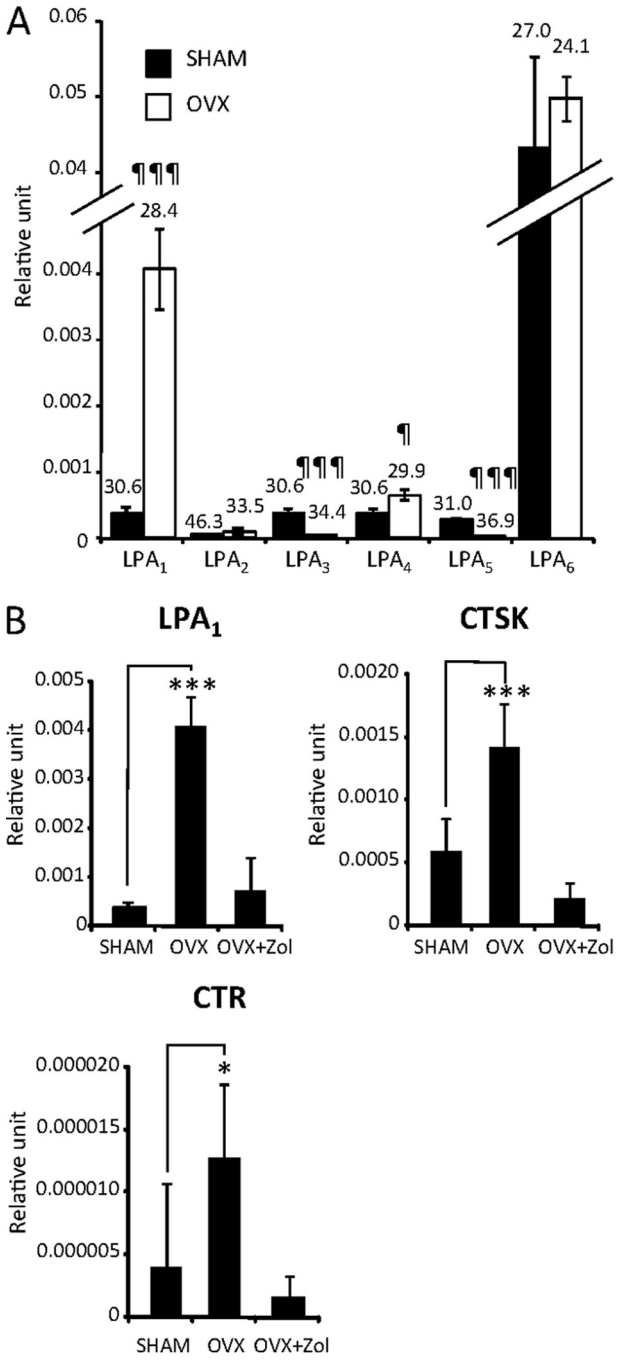

FIGURE 6. **LPA$_1$ is up-regulated in bones of ovariectomized mice.** *A,* real time PCR analysis of LPA receptor (LPA$_{1-6}$) mRNA expression in bone of OVX- and sham-operated mice. Values are the mean ± S.D. of three mice normalized to housekeeping gene *L32*. ¶, $p < 0.05$; ¶¶, $p < 0.01$; ¶¶¶, $p < 0.001$ *versus* SHAM-operated animals using two-sided unpaired *t* test. *B,* real time PCR analysis of LPA$_1$, CTR, and CTSK mRNA expression in bone of OVX- and sham-operated mice and ovariectomized mice treated with zoledronic acid (100 μg/kg) (*OVX+Zol*). Values are the mean ± S.D. of three mice normalized to housekeeping gene *L32*. All values are the mean ± S.D. of three mice. *, $p < 0.05$; ***, $p < 0.01$ *versus* SHAM-operated animals. ANOVA with Bonferroni post-test.

(Fig. 8*A*). Next we examined the effect of Debio0719 on the mobility of osteoclast precursors in live bone tissues by using intravital multiphoton microscopy (42). CX_3CR1-EGFP mice were administered with either Debio0719 (20 mg/kg) or vehicle s.c., and bone tissues were visualized to measure the mobility of EGFP$^+$ cells 4 h later (Fig. 8*B* and supplemental video 1 and video 2). The mean tracking velocity of CX_3CR1-EGFP$^+$ circulating osteoclast precursors was significantly increased in mice treated with Debio0719 (Fig. 8*C*) suggesting decreased recruitment of osteoclasts at the bone surface because of increased osteoclast precursors mobility in the marrow. Therefore, LPA$_1$ may contribute to retaining circulating osteoclast precursors in bone marrow cavity.

DISCUSSION

Bone remodeling controls bone mass through a complex regulation of the balance between bone formation mediated by osteoblasts and bone resorption through osteoclast activity (1). Here, we demonstrate that *Lpar1*$^{-/-}$ animals also display altered osteoclast differentiation and activity, indicating that LPA/LPA$_1$ pathway plays a central role in bone remodeling and the interplay between osteoblasts and osteoclasts.

LPA is a serum-borne factor required for MCSF/RANK-L-induced osteoclastogenesis of BMCs (52). Compared with previous reports describing the role of LPA on osteoclast function, our *in vitro* experiments were carried out in the presence of serum, avoiding potential LPA-independent serum stress signals on osteoclast primary culture cells. Incubating mature osteoclasts for 12 h in serum-free medium induces apoptosis that is rescued by addition of LPA, demonstrating that LPA is an osteoclast survival factor (8). However, the role of LPA in bone resorption is quite controversial and not well characterized to date. *In vitro*, LPA is shown to increase the bone resorption activity of rabbit osteoclasts but to cause a significant reduction of pits formed of mouse osteoclasts (8, 53). In our study, we found that supplementation of serum-containing medium with Ki16425 inhibited complete sealing zone formation and decreased resorption activity in mouse osteoclasts, indicating that through activation of LPA$_1$, LPA promoted bone resorption. Sealing zones are dynamic structures delineating compartments in which protons and proteases are secreted by osteoclasts to dissolve and degrade the mineralized matrix (48). Sealing zones are found in myeloid cells and are composed of cytoskeletal structures, named podosomes, that relate to stress fibers and focal adhesions in mesenchymal cells sharing similar regulation via Rho GTPases (54). LPA$_1$ was primarily identified for its capacity to induce cytoskeleton rearrangement and cell contraction through a mechanism involving $G\alpha_{12/13}$ and downstream activation of RhoA (20, 55). Therefore, acting through RhoA, LPA$_1$ may likely control complete sealing zone formation, resulting in decreased resorption activity as observed on WT osteoclasts treated with Ki16425. Mature *Lpar1*$^{-/-}$ osteoclasts showed a significant reduction of podosome belt formation and a decrease in the extent of mineral resorption, demonstrating that in the presence of serum LPA$_1$ controls osteoclastic bone resorption.

Increased cell survival, proliferation, and motility are hallmarks of LPA effects on a large range of cell types (56). Cells commonly co-express multiple LPA receptors, and defining the ones that are involved in specific functions remains challenging. Transcripts encoding LPA$_1$, LPA$_2$, LPA$_4$, and LPA$_5$ are present in mature osteoclasts (8). We found expression of LPA$_1$ at all stages of osteoclast differentiation that was further up-

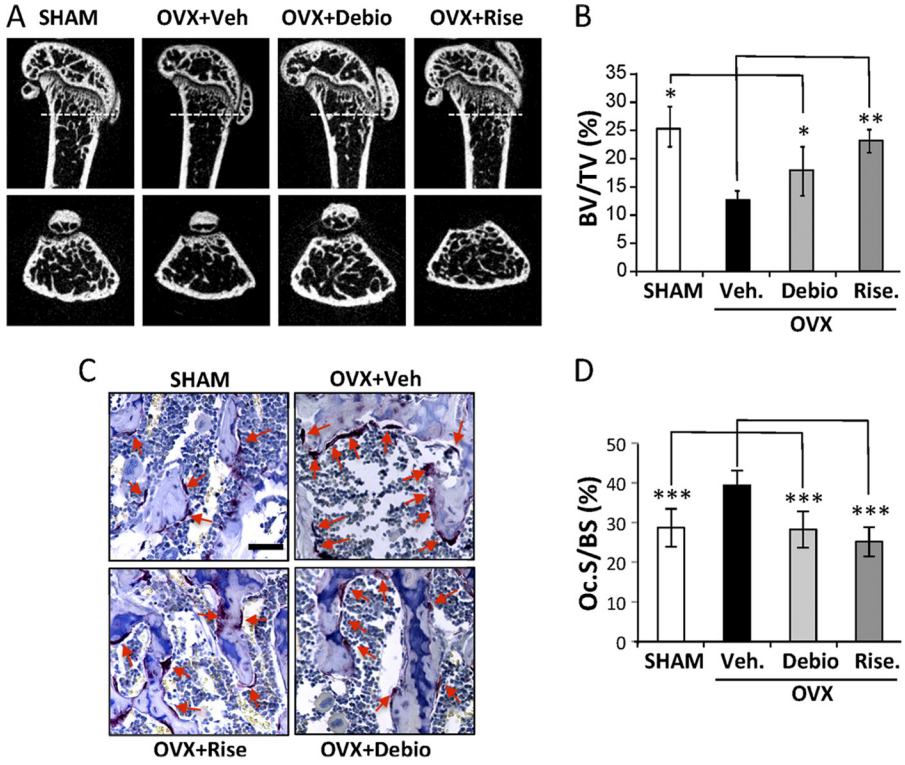

FIGURE 7. **Inhibition of LPA$_1$ activity prevents OVX-induced bone loss.** *A,* two-dimensional longitudinal (*upper panels*) and transversal (*lower panels*) sections of femurs of 9-week-old OVX or sham-operated BALB/c mice treated with vehicle (*Veh*), risedronate (*Rise*), or Debio019 (*Debio*). *Dotted lines* indicated epiphysis transversal section location. *B,* trabecular bone volume in femurs of mice 4 weeks after surgical intervention. *C,* micrographs of TRAP-stained tibia sections of sham or OVX mice treated with vehicle, risedronate, or Debio019. *Red arrows* indicate bone-lining osteoclasts. *D,* histomorphometric assessment of the resorption surface (*Oc.S/BS*) of animals in each group. All values are the mean ± S.D. of 6–8 mice. *, $p < 0.05$; **, $p < 0.01$; *** $p < 0.001$ *versus* vehicle-treated OVX mice using one-way ANOVA with Bonferroni post-test. *Bar scale,* 250 μm.

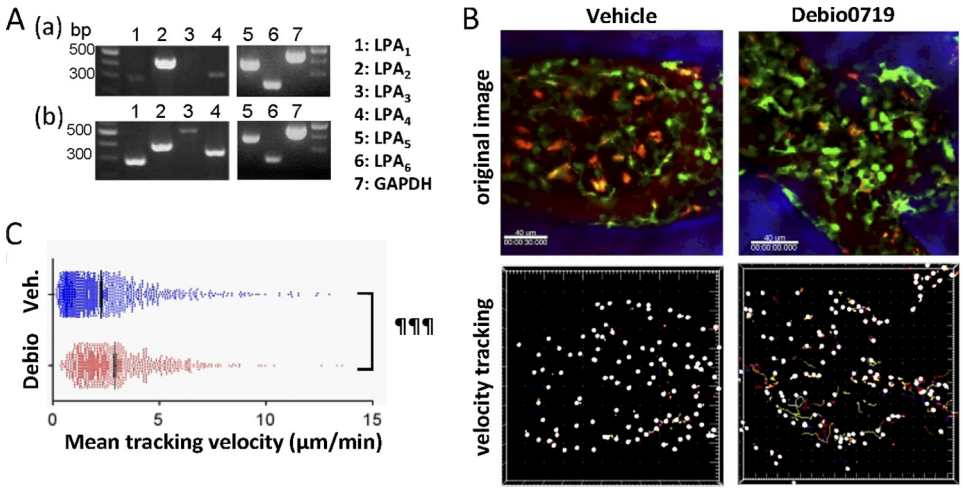

FIGURE 8. **Effect of LPA$_1$ activity inhibition on the motility of osteoclast precursors in bone.** *A,* expression of mRNA of LPA receptors in CX$_3$CR1$^+$ cells. CX$_3$CR1$^+$ cells from bone marrow in CX$_3$CR1-EGFP mice were sorted by FACS Aria, and RT-PCR was performed to detect LPA receptor and GAPDH expressions. *Panel a,* total complementary DNA isolated from mouse brain was used as a positive control (*panel b*). *B,* intravital multiphoton imaging of mouse skull bone tissues of CX$_3$CR1-EGFP mice, treated with either vehicle only (*left panels*; supplemental Video 1) or Debio0719 (*right panels*; supplemental Video 2). CX$_3$CR1$^+$ cells appear *green*. The microvasculature was visualized by intravenous injection of Texas red-conjugated 70-kDa dextran (*red*). *Blue* indicates the bone surface (*upper panels*). The movements of CX$_3$CR1$^+$ cells were tracked for 30 min. *Colored lines* show the associated trajectories of cells (*lower panels*). *Scale bars,* 40 μm. *C,* summary of the mean tracking velocity of CX$_3$CR1-EGFP cells treated with vehicle (*blue circle*) and Debio0719 (*red circle*). Data points ($n = 831$ for vehicle-treated; $n = 1163$ for Debio0719-treated) represent individual cells compiled from three independent experiments, and *error bars* represent ± S.E. ¶¶¶, $p <$ 0.001 *versus* vehicle-treated mice using two-sided unpaired *t* test.

regulated together with LPA$_2$, LPA$_4$, and LPA$_5$ concomitantly with the fusion and differentiation phases of osteoclast precursors. *Lpar2*$^{-/-}$ BMCs had not altered osteoclastogenesis capacity, suggesting that LPA$_2$ may not contribute to bone remodeling via osteoclast activity. The role of LPA$_4$, LPA$_5$, and LPA$_6$ in osteoclast function remains to be established. LPA$_1$ transduces the mitogenic activity of LPA in fibroblasts and cancer cells (57–60). Proliferation of osteoclast precursors is a prerequisite for successful osteoclastogenesis (44). Treatment of BMCs with Ki16425 during the proliferation phase of osteoclast progeni-

tors had no effect on the final number of mature osteoclasts, indicating that LPA_1 activity is not required for proliferation of osteoclast precursors. In addition, expression of c-Fos and c-Fms was not affected by Ki16425 treatment. RANK-L activates expression of c-Fos (61), and high concentrations of MCSF acting through c-Fms restores the expression of c-Fos in *Beta3*$^{-/-}$ osteoclasts (62). Therefore, although LPA up-regulates c-Fos in various cells (63), its expression in osteoclasts was likely sustained by MCSF and RANK-L abundantly present in BMC culture media independently of LPA action. LPA activates NFATc1 in osteoclasts and promotes survival (8). Decreased expression of NFATc1 in BMCs treated with Ki16425 might decrease osteoclast precursor survival and differentiation and together with decreased expression of the fusion protein DC-STAMP could be responsible for the observed decrease in the fusion of osteoclast precursors.

LPA_1 is the most ubiquitous LPA receptor (64). Expression of LPA_1 in bone cells is well documented (65). However, regulation of LPA_1 expression in bone is not known. OVX or continuous exposure to elevated levels of PTH results in an increase in bone resorption activity, hypercalcemia, and bone loss (66, 67), whereas subcutaneous intermittent PTH administration increases bone turnover and osteoblast activity resulting in net anabolic effects on bone and reduced risk of fractures (68). *Lpar1* expression was not reported in the list of genes that were modulated in the bones of animals treated with intermittent administration of PTH (69), whereas *Lpar1* was up-regulated by 1.5-fold in the bone of rats treated with continuous infusion of PTH(1–34) (70). We found *Lpar1* was up-regulated by 4-fold in the bones of ovariectomized mice. These results strongly support the link between LPA_1 expression and osteoclast activity *in vivo*. Aminobisphosphonates (*i.e.* zoledronic acid and risedronate) are powerful inhibitors of osteoclast activity and thereby are the standard of care in patients with diseases associated with excessive bone resorption, such as osteoporosis, multiple myeloma, and bone metastases (71). Here, we showed that zoledronic acid inhibited up-regulation of LPA_1 in bones of ovariectomized mice, confirming that modulation of LPA_1 expression was linked to mature osteoclast activity. Blocking LPA_1 function *in vivo* with the LPA_1 antagonist Ki16425 inhibits the progression of osteolytic bone lesions in mouse models (72). The Ki16425 structurally related LPA_1 antagonist, Debio0719 (38), partially prevented bone loss induced by OVX compared with complete bone loss prevention with risedronate. Remarkably, Debio0719 was equally potent as risedronate at inhibiting the increase of osteoclast number at the bone surface of ovariectomized mice, but the underlying mechanisms may be different. Nitrogen-containing bisphosphonates are powerful inducers of apoptosis of osteoclasts due to inhibition of farnesyl pyrophosphate synthase activity (73). *In vivo*, resorbing osteoclasts undergo apoptosis due to uptake of bisphosphonate released from the bone surface. We demonstrate that antagonists of LPA_1 decreased *in vitro* osteoclast differentiation and *in vivo* the number of osteoclasts lining on the surface of trabecular bone of ovariectomized mice. Osteoclast precursors are nonadherent circulating hematopoietic cells (44). *In vivo* osteoclastogenesis depends on the recruitment and attachment of osteoclast progenitors to the bone surface initiating their fusion and subsequent differentiation. Our *in vitro* results demonstrate that blocking the LPA_1 pathway inhibits the expression of osteoclast markers, including the adhesion molecule β3 integrin, and the fusion of osteoclast precursors, and interferes with the cytoskeletal organization altering adhesion of mature osteoclasts to mineralized surfaces. Debio0719 reduces the number of osteoclasts attached to the bone surface in ovariectomized mice. The mode of action of Debio0719 *in vivo* was not completely determined but may include the inhibition of osteoclast differentiation and a decrease in the attachment of osteoclast precursors to the bone matrix. A reduced residence time of the nonadherent osteoclast progenitors at the bone surface combined with an increased motility of CX_3CR1-GFP osteoclast precursors would decrease the number of fusion events and therefore the number of osteoclasts at the bone surface. Subsequently, the number of nonadherent osteoclast precursors floating in bone marrow would be increased. This hypothesis was supported by the increase in CX_3CR1-GFP$^+$ nonadherent osteoclast progenitor mean tracking velocity in the bone marrow of animals treated with Debio0719. However, the contribution of other LPA receptors (*i.e.* LPA_{4-6}) to this phenomenon remains to be established. Nevertheless, bone mass recovery of ovariectomized mice treated with Debio0719 (50 mg/kg) was not complete. This may be a result of an inhibitory effect of the treatment on bone formation as the use of LPA_1 antagonists also inhibits osteoblast differentiation *in vitro* (7, 74). Therefore, it is conceivable that systemic treatment with Debio0719 may inhibit overall bone remodeling by affecting both osteoclast and osteoblast function, thus decreasing bone resorption while limiting bone formation.

Overall, our results demonstrate that LPA_1 controls bone remodeling by regulating directly osteoclastogenesis and motility of osteoclast precursors *in vivo* and bone resorption. We have shown previously that LPA_1 is a potential target in the context of osteolytic bone metastases (72). A recent work showed that blocking LPA_1 inhibits the development of arthritis via cellular infiltration, Th17 differentiation, and osteoclastogenesis (75). Our study extends the field of applications of anti-LPA_1 therapy for patients suffering from bone fragility disorders due to excessive bone resorption.

Acknowledgments—Debio0719 was generously provided by Debiopharm S.A. (Lausanne, Switzerland). We thank J. M. Vicat (Animalerie Lyon Est Conventionnelle et Specific Pathogen Free (ALECS-SPF) Animal Care Facility, UCBL, Lyon France) for technical support.

REFERENCES

1. Rodan, G. A., and Martin, T. J. (2000) Therapeutic approaches to bone diseases. *Science* **289,** 1508–1514
2. Jacobs, C. R., Temiyasathit, S., and Castillo, A. B. (2010) Osteocyte mechanobiology and pericellular mechanics. *Annu. Rev. Biomed. Eng.* **12,** 369–400
3. Nakashima, T., Hayashi, M., and Takayanagi, H. (2012) New insights into osteoclastogenic signaling mechanisms. *Trends Endocrinol. Metab.* **23,** 582–590
4. Takeda, S., and Karsenty, G. (2001) Central control of bone formation. *J. Bone Miner. Metab.* **19,** 195–198
5. Nakamura, T., Imai, Y., Matsumoto, T., Sato, S., Takeuchi, K., Igarashi, K., Harada, Y., Azuma, Y., Krust, A., Yamamoto, Y., Nishina, H., Takeda, S.,

Takayanagi, H., Metzger, D., Kanno, J., Takaoka, K., Martin, T. J., Chambon, P., and Kato, S. (2007) Estrogen prevents bone loss via estrogen receptor α and induction of Fas ligand in osteoclasts. *Cell* **130,** 811–823
6. Houben, A. J., and Moolenaar, W. H. (2011) Autotaxin and LPA receptor signaling in cancer. *Cancer Metastasis Rev.* **30,** 557–565
7. Mansell, J. P., Nowghani, M., Pabbruwe, M., Paterson, I. C., Smith, A. J., and Blom, A. W. (2011) Lysophosphatidic acid and calcitriol co-operate to promote human osteoblastogenesis: requirement of albumin-bound LPA. *Prostaglandins Other Lipid Mediat.* **95,** 45–52
8. Lapierre, D. M., Tanabe, N., Pereverzev, A., Spencer, M., Shugg, R. P., Dixon, S. J., and Sims, S. M. (2010) Lysophosphatidic acid signals through multiple receptors in osteoclasts to elevate cytosolic calcium concentration, evoke retraction, and promote cell survival. *J. Biol. Chem.* **285,** 25792–25801
9. Karagiosis, S. A., and Karin, N. J. (2007) Lysophosphatidic acid induces osteocyte dendrite outgrowth. *Biochem. Biophys. Res. Commun.* **357,** 194–199
10. Moolenaar, W. H. (2000) Development of our current understanding of bioactive lysophospholipids. *Ann. N.Y. Acad. Sci.* **905,** 1–10
11. Eichholtz, T., Jalink, K., Fahrenfort, I., and Moolenaar, W. H. (1993) The bioactive phospholipid lysophosphatidic acid is released from activated platelets. *Biochem. J.* **291,** 677–680
12. Boucharaba, A., Serre, C.-M., Grès, S., Saulnier-Blache, J. S., Bordet, J.-C., Guglielmi, J., Clézardin, P., and Peyruchaud, O. (2004) Platelet-derived lysophosphatidic acid supports the progression of osteolytic bone metastases in breast cancer. *J. Clin. Invest.* **114,** 1714–1725
13. Panupinthu, N., Rogers, J. T., Zhao, L., Solano-Flores, L. P., Possmayer, F., Sims, S. M., and Dixon, S. J. (2008) P2X7 receptors on osteoblasts couple to production of lysophosphatidic acid: a signaling axis promoting osteogenesis. *J. Cell Biol.* **181,** 859–871
14. Choi, J. W., Herr, D. R., Noguchi, K., Yung, Y. C., Lee, C. W., Mutoh, T., Lin, M. E., Teo, S. T., Park, K. E., Mosley, A. N., and Chun, J. (2010) LPA receptors: subtypes and biological actions. *Annu. Rev. Pharmacol. Toxicol.* **50,** 157–186
15. Mutoh, T., Rivera, R., and Chun, J. (2012) Insights into the pharmacological relevance of lysophospholipid receptors. *Br. J. Pharmacol.* **165,** 829–844
16. Noguchi, K., Herr, D., Mutoh, T., and Chun, J. (2009) Lysophosphatidic acid (LPA) and its receptors. *Curr. Opin. Pharmacol.* **9,** 15–23
17. Choi, K. U., Yun, J. S., Lee, I. H., Heo, S. C., Shin, S. H., Jeon, E. S., Choi, Y. J., Suh, D. S., Yoon, M. S., and Kim, J. H. (2010) Lysophosphatidic acid-induced expression of periostin in stromal cells: Prognostic relevance of periostin expression in epithelial ovarian cancer. *Int. J. Cancer* **128,** 332–342
18. Sims, S. M., Panupinthu, N., Lapierre, D. M., Pereverzev, A., and Dixon, S. J. (2013) Lysophosphatidic acid: A potential mediator of osteoblast-osteoclast signaling in bone. *Biochim. Biophys. Acta* **1831,** 109–116
19. Contos, J. J., Fukushima, N., Weiner, J. A., Kaushal, D., and Chun, J. (2000) Requirement for the lpA1 lysophosphatidic acid receptor gene in normal suckling behavior. *Proc. Natl. Acad. Sci. U.S.A.* **97,** 13384–13389
20. Hecht, J. H., Weiner, J. A., Post, S. R., and Chun, J. (1996) Ventricular zone gene-1 (vzg-1) encodes a lysophosphatidic acid receptor expressed in neurogenic regions of the developing cerebral cortex. *J. Cell Biol.* **135,** 1071–1083
21. Kingsbury, M. A., Rehen, S. K., Contos, J. J., Higgins, C. M., and Chun, J. (2003) Non-proliferative effects of lysophosphatidic acid enhance cortical growth and folding. *Nat. Neurosci.* **6,** 1292–1299
22. Inoue, M., Rashid, M. H., Fujita, R., Contos, J. J., Chun, J., and Ueda, H. (2004) Initiation of neuropathic pain requires lysophosphatidic acid receptor signaling. *Nat. Med.* **10,** 712–718
23. Yung, Y. C., Mutoh, T., Lin, M. E., Noguchi, K., Rivera, R. R., Choi, J. W., Kingsbury, M. A., and Chun, J. (2011) Lysophosphatidic acid signaling may initiate fetal hydrocephalus. *Sci. Transl. Med.* **3,** 99ra87
24. Tager, A. M., LaCamera, P., Shea, B. S., Campanella, G. S., Selman, M., Zhao, Z., Polosukhin, V., Wain, J., Karimi-Shah, B. A., Kim, N. D., Hart, W. K., Pardo, A., Blackwell, T. S., Xu, Y., Chun, J., and Luster, A. D. (2008) The lysophosphatidic acid receptor LPA(1) links pulmonary fibrosis to lung injury by mediating fibroblast recruitment and vascular leak. *Nat. Med.* **14,** 45–54
25. Lin, S., Yeruva, S., He, P., Singh, A. K., Zhang, H., Chen, M., Lamprecht, G., de Jonge, H. R., Tse, M., Donowitz, M., Hogema, B. M., Chun, J., Seidler, U., and Yun, C. C. (2010) Lysophosphatidic acid stimulates the intestinal brush border Na^+/H^+ exchanger 3 and fluid absorption via LPA(5) and NHERF2. *Gastroenterology* **138,** 649–658
26. Panchatcharam, M., Miriyala, S., Yang, F., Rojas, M., End, C., Vallant, C., Dong, A., Lynch, K., Chun, J., Morris, A. J., and Smyth, S. S. (2008) Lysophosphatidic acid receptors 1 and 2 play roles in regulation of vascular injury responses but not blood pressure. *Circ. Res.* **103,** 662–670
27. Dusaulcy, R., Daviaud, D., Pradère, J. P., Grès, S., Valet, P., and Saulnier-Blache, J. S. (2009) Altered food consumption in mice lacking lysophosphatidic acid receptor-1. *J. Physiol. Biochem.* **65,** 345–350
28. Gennero, I., Laurencin-Dalicieux, S., Conte-Auriol, F., Briand-Mésange, F., Laurencin, D., Rue, J., Beton, N., Malet, N., Mus, M., Tokumura, A., Bourin, P., Vico, L., Brunel, G., Oreffo, R. O., Chun, J., and Salles, J. P. (2011) Absence of the lysophosphatidic acid receptor LPA1 results in abnormal bone development and decreased bone mass. *Bone* **49,** 395–403
29. Contos, J. J., Ishii, I., Fukushima, N., Kingsbury, M. A., Ye, X., Kawamura, S., Brown, J. H., and Chun, J. (2002) Characterization of lpa(2) (Edg4) and lpa(1)/lpa(2) (Edg2/Edg4) lysophosphatidic acid receptor knockout mice: signaling deficits without obvious phenotypic abnormality attributable to lpa(2). *Mol. Cell. Biol.* **22,** 6921–6929
30. Ye, X., Hama, K., Contos, J. J., Anliker, B., Inoue, A., Skinner, M. K., Suzuki, H., Amano, T., Kennedy, G., Arai, H., Aoki, J., and Chun, J. (2005) LPA3-mediated lysophosphatidic acid signalling in embryo implantation and spacing. *Nature* **435,** 104–108
31. Ye, X., Skinner, M. K., Kennedy, G., and Chun, J. (2008) Age-dependent loss of sperm production in mice via impaired lysophosphatidic acid signaling. *Biol. Reprod.* **79,** 328–336
32. Sumida, H., Noguchi, K., Kihara, Y., Abe, M., Yanagida, K., Hamano, F., Sato, S., Tamaki, K., Morishita, Y., Kano, M. R., Iwata, C., Miyazono, K., Sakimura, K., Shimizu, T., and Ishii, S. (2010) LPA4 regulates blood and lymphatic vessel formation during mouse embryogenesis. *Blood* **116,** 5060–5070
33. Liu, Y. B., Kharode, Y., Bodine, P. V., Yaworsky, P. J., Robinson, J. A., and Billiard, J. (2010) LPA induces osteoblast differentiation through interplay of two receptors: LPA1 and LPA4. *J. Cell. Biochem.* **109,** 794–800
34. Lin, M. E., Rivera, R. R., and Chun, J. (2012) Targeted deletion of LPA5 identifies novel roles for lysophosphatidic acid signaling in development of neuropathic pain. *J. Biol. Chem.* **287,** 17608–17617
35. An, S., Bleu, T., Hallmark, O. G., and Goetzl, E. J. (1998) Characterization of a novel subtype of human G protein-coupled receptor for lysophosphatidic acid. *J. Biol. Chem.* **273,** 7906–7910
36. Heise, C. E., Santos, W. L., Schreihofer, A. M., Heasley, B. H., Mukhin, Y. V., Macdonald, T. L., and Lynch, K. R. (2001) Activity of 2-substituted lysophosphatidic acid (LPA) analogs at LPA receptors: discovery of a LPA1/LPA3 receptor antagonist. *Mol. Pharmacol.* **60,** 1173–1180
37. Ohta, H., Sato, K., Murata, N., Damirin, A., Malchinkhuu, E., Kon, J., Kimura, T., Tobo, M., Yamazaki, Y., Watanabe, T., Yagi, M., Sato, M., Suzuki, R., Murooka, H., Sakai, T., Nishitoba, T., Im, D. S., Nochi, H., Tamoto, K., Tomura, H., and Okajima, F. (2003) Ki16425, a subtype-selective antagonist for EDG-family lysophosphatidic acid receptors. *Mol. Pharmacol.* **64,** 994–1005
38. David, M., Ribeiro, J., Descotes, F., Serre, C. M., Barbier, M., Murone, M., Clézardin, P., and Peyruchaud, O. (2012) Targeting lysophosphatidic acid receptor type 1 with Debio 0719 inhibits spontaneous metastasis dissemination of breast cancer cells independently of cell proliferation and angiogenesis. *Int. J. Oncol.* **40,** 1133–1141
39. Lee, C. W., Rivera, R., Gardell, S., Dubin, A. E., and Chun, J. (2006) GPR92 as a new $G_{12/13}$- and G_q-coupled lysophosphatidic acid receptor that increases cAMP, LPA5. *J. Biol. Chem.* **281,** 23589–23597
40. Yanagida, K., Masago, K., Nakanishi, H., Kihara, Y., Hamano, F., Tajima, Y., Taguchi, R., Shimizu, T., and Ishii, S. (2009) Identification and characterization of a novel lysophosphatidic acid receptor, p2y5/LPA6. *J. Biol. Chem.* **284,** 17731–17741
41. Jung, S., Aliberti, J., Graemmel, P., Sunshine, M. J., Kreutzberg, G. W., Sher, A., and Littman, D. R. (2000) Analysis of fractalkine receptor

CX(3)CR1 function by targeted deletion and green fluorescent protein reporter gene insertion. *Mol. Cell. Biol.* **20,** 4106–4114
42. Ishii, M., Egen, J. G., Klauschen, F., Meier-Schellersheim, M., Saeki, Y., Vacher, J., Proia, R. L., and Germain, R. N. (2009) Sphingosine-1-phosphate mobilizes osteoclast precursors and regulates bone homeostasis. *Nature* **458,** 524–528
43. Schmittgen, T. D., and Livak, K. J. (2008) Analyzing real-time PCR data by the comparative C(T) method. *Nat. Protoc.* **3,** 1101–1108
44. Teitelbaum, S. L., and Ross, F. P. (2003) Genetic regulation of osteoclast development and function. *Nat. Rev. Genet.* **4,** 638–649
45. Lattin, J., Zidar, D. A., Schroder, K., Kellie, S., Hume, D. A., and Sweet, M. J. (2007) G-protein-coupled receptor expression, function, and signaling in macrophages. *J. Leukocyte Biol.* **82,** 16–32
46. Fueller, M., Wang, D. A., Tigyi, G., and Siess, W. (2003) Activation of human monocytic cells by lysophosphatidic acid and sphingosine-1-phosphate. *Cell. Signal.* **15,** 367–375
47. Duong, C. Q., Bared, S. M., Abu-Khader, A., Buechler, C., Schmitz, A., and Schmitz, G. (2004) Expression of the lysophospholipid receptor family and investigation of lysophospholipid-mediated responses in human macrophages. *Biochim. Biophys. Acta* **1682,** 112–119
48. Jurdic, P., Saltel, F., Chabadel, A., and Destaing, O. (2006) Podosome and sealing zone: specificity of the osteoclast model. *Eur. J. Cell Biol.* **85,** 195–202
49. Zhang, Q., Magnusson, M. K., and Mosher, D. F. (1997) Lysophosphatidic acid and microtubule-destabilizing agents stimulate fibronectin matrix assembly through Rho-dependent actin stress fiber formation and cell contraction. *Mol. Biol. Cell* **8,** 1415–1425
50. Kalu, D. N. (1991) The ovariectomized rat model of postmenopausal bone loss. *Bone Miner.* **15,** 175–191
51. Rissanen, J. P., Suominen, M. I., Peng, Z., and Halleen, J. M. (2008) Secreted tartrate-resistant acid phosphatase 5b is a marker of osteoclast number in human osteoclast cultures and the rat ovariectomy model. *Calcif. Tissue Int.* **82,** 108–115
52. David, M., Wannecq, E., Descotes, F., Jansen, S., Deux, B., Ribeiro, J., Serre, C. M., Grès, S., Bendriss-Vermare, N., Bollen, M., Saez, S., Aoki, J., Saulnier-Blache, J. S., Clézardin, P., and Peyruchaud, O. (2010) Cancer cell expression of autotaxin controls bone metastasis formation in mouse through lysophosphatidic acid-dependent activation of osteoclasts. *PLoS ONE* **5,** e9741
53. McMichael, B. K., Meyer, S. M., and Lee, B. S. (2010) c-Src-mediated phosphorylation of thyroid hormone receptor-interacting protein 6 (TRIP6) promotes osteoclast sealing zone formation. *J. Biol. Chem.* **285,** 26641–26651
54. Ory, S., Brazier, H., Pawlak, G., and Blangy, A. (2008) Rho GTPases in osteoclasts: orchestrators of podosome arrangement. *Eur. J. Cell Biol.* **87,** 469–477
55. Fukushima, N., Kimura, Y., and Chun, J. (1998) A single receptor encoded by vzg-1/lpA1/edg-2 couples to G proteins and mediates multiple cellular responses to lysophosphatidic acid. *Proc. Natl. Acad. Sci. U.S.A.* **95,** 6151–6156
56. Moolenaar, W. H., Kranenburg, O., Postma, F. R., and Zondag, G. C. (1997) Lysophosphatidic acid: G-protein signalling and cellular responses. *Curr. Opin. Cell Biol.* **9,** 168–173
57. Yu, S., Murph, M. M., Lu, Y., Liu, S., Hall, H. S., Liu, J., Stephens, C., Fang, X., and Mills, G. B. (2008) Lysophosphatidic acid receptors determine tumorigenicity and aggressiveness of ovarian cancer cells. *J. Natl. Cancer Inst.* **100,** 1630–1642
58. Daaka, Y. (2002) Mitogenic action of LPA in prostate. *Biochim. Biophys. Acta* **1582,** 265–269
59. Boucharaba, A., Guillet, B., Menaa, F., Hneino, M., van Wijnen, A. J., Clézardin, P., Philippe, C., Peyruchaud, O., and Oliver, P. (2009) Bioactive lipids lysophosphatidic acid and sphingosine 1-phosphate mediate breast cancer cell biological functions through distinct mechanisms. *Oncol. Res.* **18,** 173–184
60. Sakai, N., Chun, J., Duffield, J. S., Wada, T., Luster, A. D., and Tager, A. M. (2013) LPA1-induced cytoskeleton reorganization drives fibrosis through CTGF-dependent fibroblast proliferation. *FASEB J***27,** 1830–1846
61. Takayanagi, H. (2007) Osteoimmunology: shared mechanisms and crosstalk between the immune and bone systems. *Nat. Rev. Immunol.* **7,** 292–304
62. Faccio, R., Takeshita, S., Zallone, A., Ross, F. P., and Teitelbaum, S. L. (2003) c-Fms and the $\alpha v\beta 3$ integrin collaborate during osteoclast differentiation. *J. Clin. Invest.* **111,** 749–758
63. Spencer, J. A., and Misra, R. P. (1999) Expression of the SRF gene occurs through a Ras/Sp/SRF-mediated-mechanism in response to serum growth signals. *Oncogene* **18,** 7319–7327
64. Lin, M. E., Herr, D. R., and Chun, J. (2010) Lysophosphatidic acid (LPA) receptors: signaling properties and disease relevance. *Prostaglandins Other Lipid Mediat.* **91,** 130–138
65. Peyruchaud, O., Leblanc, R., and David, M. (2013) Pleiotropic activity of lysophosphatidic acid in bone metastasis. *Biochim. Biophys. Acta* **1831,** 99–104
66. Marx, U. C., Adermann, K., Bayer, P., Forssmann, W. G., and Rösch, P. (2000) Solution structures of human parathyroid hormone fragments hPTH(1–34) and hPTH(1–39) and bovine parathyroid hormone fragment bPTH(1–37). *Biochem. Biophys. Res. Commun.* **267,** 213–220
67. Wysolmerski, J. J. (2012) Parathyroid hormone-related protein: an update. *J. Clin. Endocrinol. Metab.* **97,** 2947–2956
68. Delmas, P. D., Vergnaud, P., Arlot, M. E., Pastoureau, P., Meunier, P. J., and Nilssen, M. H. (1995) The anabolic effect of human PTH(1–34) on bone formation is blunted when bone resorption is inhibited by the bisphosphonate tiludronate–is activated resorption a prerequisite for the *in vivo* effect of PTH on formation in a remodeling system? *Bone* **16,** 603–610
69. Ferrari, S. L., Pierroz, D. D., Glatt, V., Goddard, D. S., Bianchi, E. N., Lin, F. T., Manen, D., and Bouxsein, M. L. (2005) Bone response to intermittent parathyroid hormone is altered in mice null for β-arrestin2. *Endocrinology* **146,** 1854–1862
70. Onyia, J. E., Helvering, L. M., Gelbert, L., Wei, T., Huang, S., Chen, P., Dow, E. R., Maran, A., Zhang, M., Lotinun, S., Lin, X., Halladay, D. L., Miles, R. R., Kulkarni, N. H., Ambrose, E. M., Ma, Y. L., Frolik, C. A., Sato, M., Bryant, H. U., and Turner, R. T. (2005) Molecular profile of catabolic versus anabolic treatment regimens of parathyroid hormone (PTH) in rat bone: an analysis by DNA microarray. *J. Cell. Biochem.* **95,** 403–418
71. Coleman, R. (2011) The use of bisphosphonates in cancer treatment. *Ann. N.Y. Acad. Sci.* **1218,** 3–14
72. Boucharaba, A., Serre, C. M., Guglielmi, J., Bordet, J. C., Clézardin, P., and Peyruchaud, O. (2006) The type 1 lysophosphatidic acid receptor is a target for therapy in bone metastases. *Proc. Natl. Acad. Sci. U.S.A.* **103,** 9643–9648
73. Rogers, M. J. (2003) New insights into the molecular mechanisms of action of bisphosphonates. *Curr. Pharm. Des.* **9,** 2643–2658
74. Gidley, J., Openshaw, S., Pring, E. T., Sale, S., and Mansell, J. P. (2006) Lysophosphatidic acid cooperates with 1α,25(OH)2D3 in stimulating human MG63 osteoblast maturation. *Prostaglandins Other Lipid Mediat.* **80,** 46–61
75. Miyabe, Y., Miyabe, C., Iwai, Y., Takayasu, A., Fukuda, S., Yokoyama, W., Nagai, J., Jona, M., Tokuhara, Y., Ohkawa, R., Albers, H. M., Ovaa, H., Aoki, J., Chun, J., Yatomi, Y., Ueda, H., Miyasaka, M., Miyasaka, N., and Nanki, T. (2013) Necessity of lysophosphatidic acid receptor 1 for development of arthritis. *Arthritis Rheum.* **65,** 2037–2047